Spontaneous separation of bi-stable biochemical systems into spatial domains of opposite phases

J. Elf[†] and M. Ehrenberg

Abstract: Bi-stable chemical systems are the basic building blocks for intracellular memory and cell fate decision circuits. These circuits are built from molecules, which are present at low copy numbers and are slowly diffusing in complex intracellular geometries. The stochastic reaction-diffusion kinetics of a double-negative feedback system and a MAPK phosphorylation-dephosphorylation system is analysed with Monte-Carlo simulations of the reaction-diffusion master equation. The results show the geometry of intracellular reaction compartments to be important both for the duration and the locality of biochemical memory. Rules for when the systems lose global hysteresis by spontaneous separation into spatial domains in opposite phases are formulated in terms of geometrical constraints, diffusion rates and attractor escape times. The analysis is facilitated by a new efficient algorithm for exact sampling of the Markov process corresponding to the reaction-diffusion master equation.

1 Introduction

Biochemical systems can be in different, self-perpetuating states depending on previous stimuli [1–3]. Such biochemical memory is exemplified by the irreversible developmental switches in the cell cycle [4], the maturation of oocytes [5], the on-off switches in gene-activity [6], and the ubiquitous phosphorylation switches in signal transduction pathways [7]. The dynamical properties of such systems often defy intuition, and their analysis requires mathematical modelling [8]. To account for random transitions between states, stochastic descriptions of the chemical reactions are necessary [9, 10] and to account for the cell geometry and slow intracellular diffusion, spatial considerations are mandatory [11, 12]. In a recent experimental study [13] it was demonstrated that bistability can vanish due to spatially localised fluctuations for inorganic catalysts, and thus invalidate any macroscopic description of the kinetics. The present study addresses consequences of similar kinetic behaviour in intracellular biochemical systems.

Two bi-stable model systems serve to exemplify the stochastic and spatial aspects of intracellular signalling. The results reveal that the average times for random transitions between two self-perpetuating states are reduced by finite diffusion rates, and suggest a general rule for the spontaneous emergence of spatial domains in opposite states and loss of global bistability. The findings disclose previously unknown physical constraints on the design of intracellular control circuits that depend on stable attractors, and fill a gap in the current knowledge of spatially heterogeneous bi-stable systems.

Stochastic models for intracellular kinetics are gaining in importance for the interpretation of in vivo experiments [14, 15]. These models are commonly based on the homogeneous chemical master equation (ME) for well stirred systems [10, 16]. This approximation, where the state of the system is defined by the total copy numbers of the different reactants, is only valid if equilibration between the microstates of the reactants, thermal equilibration between the reactants and the solvent, and equilibration of the reactants between all positions in the system volume occur on a much faster timescale than the chemical reactions [10].

Since diffusion of molecules in a living cell is considerably slower than in the test tube [17], the condition of spatial homogeneity is expected to be violated in many cases. In fact, many important intracellular processes depend on spatial heterogeneity [11, 12]. Among these are cell division [18], morphogenesis [19], local signal processing in neurons [20], and some types of chemotaxis [21].

A feasible starting point for stochastic descriptions of spatially heterogeneous systems is to divide the reaction volume into a finite number of subvolumes and apply the reaction diffusion master equation (RDME or multivariate master equation) [9, 22, 23]. The state of such a system is defined by the copy numbers of all reactants in each artificial subvolume, which must be chosen small enough to ensure homogeneity [23]. Diffusion is accounted for as first-order elementary reactions for the exchange of molecules between subvolumes. The rate constants are D/l^2, where D is the diffusion constant for a particular reactant and l is the side length of the cubic subvolume [9, 23].

Stochastic analyses of spatially extended bi-stable systems are difficult for two reasons. Firstly, the complexity of the RDMEs makes analytical solutions hard to come by and secondly, direct numerical solutions are impossible due to the large state space. Accordingly, there exists but a handful of RDME descriptions of bi-stable non-equilibrium systems in 1D [23, 24], and none in 2D or 3D, where the most interesting biological problems reside. Furthermore, the properties of bi-stable systems in 2D and 3D cannot be inferred from 1D considerations. The reason is that curvature of domain fronts, which is important for macroscopic system dynamics in 2D and 3D [25, 26], is missing in 1D.

The present RDME-analysis of stochastic reaction diffusion kinetics in 3D was made possible by the

IEE online no. 20045022

doi: 10.1049/sb:20045022

Paper first received 16th July and in revised form 4th September 2004

The authors are with the Department of Cell and Molecular Biology, Box 596, Uppsala University, Uppsala, Sweden, [†]email: johan.elf@icm.uu.se

development of a new algorithm, the Next Subvolume Method (NSM), which is described in the next Section.

2 Results

2.1 The Next Subvolume Method

When the chemical reactions in an intracellular 3D system are fast in relation to diffusion, the subvolumes used in the RDME must be small and their number correspondingly large (several millions) to ensure spatial homogeneity of the reactants in the subvolumes on the time scale of the chemical reactions. In such cases, direct application of Gillespie's algorithm [27] for Monte Carlo simulations of the ME is not feasible, due to the linear relation that exists between the number of subvolumes and the computational effort. This has prevented such approaches to 2D and 3D systems, while 1D simulations of the RDME were pioneered already in 1979 [28]. Progress in stochastic simulations of 3D biological systems was reached in the SmartCell project [29–31] by the application of the Next Reaction Method [32] to spatial problems.

We have designed an efficient MC algorithm, the Next Subvolume Method (NSM), that samples trajectories of the Markov process corresponding to the RDME (see Supplementary Methods). The trajectories are therefore equivalent to those obtained with Gillespie's Direct Method [27]. The algorithm has been tailor-made for the RDME and the computation times scale logarithmically, rather than linearly, with the number of subvolumes. Accordingly, statistically significant results for systems that require millions of subvolumes can now be obtained with standard PCs. This leap in computational efficiency originates in a combination of the Direct Method [27] for sampling the time for a next reaction or diffusion event in each subvolume, with Gibson and Bruck's Next Reaction Method [32], which is used to keep track of in which subvolume an event occurs next. The subvolumes are kept sorted in a queue, implemented as a binary tree, according to increasing time of the next event. When an event has occurred in the subvolume at the top of the queue, new event times need to be sampled only for one (the event is a chemical reaction) or two (the event is a diffusion jump) subvolume(s).

When the number of subvolumes is large, the NSM is more efficient than a direct application of the Next Reaction Method (NRM) to the RDME (see Supplementary Methods).

2.2 Spontaneous domain separation in bi-stable systems with slow diffusion

We first analyse a bi-stable biochemical system built on the double-negative feedback principle [2]. Two enzymes, E_A and E_B, synthesise two different compounds, A and B, respectively. The A molecules inhibit the activity of E_B and the B molecules inhibit the activity of E_A. Free A and B molecules are eliminated with the same first-order rate constant. When E_A and E_B have the same kinetic parameters, the system is symmetric with respect to A and B.

$$E_A \xrightarrow{k_1} E_A + A \qquad E_B \xrightarrow{k_1} E_B + B$$

$$E_A + B \underset{k_d}{\overset{k_a}{\rightleftharpoons}} E_AB \qquad E_AB + B \underset{k_d}{\overset{k_a}{\rightleftharpoons}} E_AB_2 \qquad B \xrightarrow{k_4} \emptyset$$

$$E_B + A \underset{k_d}{\overset{k_a}{\rightleftharpoons}} E_BA \qquad E_BA + A \underset{k_d}{\overset{k_a}{\rightleftharpoons}} E_BA_2 \qquad A \xrightarrow{k_4} \emptyset$$

The double-negative feedback scheme. In the limit of fast diffusion, the parameters used in this study are: $[E_A]_{tot} = [E_B]_{tot} = 12.3\,\text{nM}$ (200 molecules in 27 femtoliters), $k_1 = 150\,\text{s}^{-1}$, $k_a = 1.2 \cdot 10^8\,\text{s}^{-1}\,\text{M}^{-1}$, $k_d = 10\,\text{s}^{-1}$, $k_4 = 6\,\text{s}^{-1}$. The RDME and the macroscopic reaction diffusion equations for the scheme are given in the online supplementary text A. The total system volume and diffusion rates are varied as described in the text. The diffusion constant, D, is set equal for all components and all reactions given in the scheme are approximated as single-step transitions. Association and dissociation rate constants are partially diffusion controlled [33], meaning that they increase towards asymptotes with increasing diffusion constants. At finite diffusion rates, the association and disassociation rate constants were modified accordingly (see online supplementary text B). The inevitable coupling between free diffusion and chemical kinetics makes it difficult to simplify detailed reaction schemes without distorting the overall properties of the system or making physically unsound assumptions.

In Fig. 1*a*, the correlation time (τ_c) for the number n_A of A molecules is plotted as a function of the linear extension of the system for different diffusion constants. τ_c is the time τ at which the normalised autocorrelation function $\langle n_A(t)n_A(t+\tau)\rangle / \langle n_A\rangle^2 - 1$ has decreased to e^{-1} of its value at $\tau = 0$. (The correlation time is one-half of the average time of escape from one of the attractors in a symmetric bistable system). When diffusion is infinitely fast, so that the system is homogenous and can be described by the ordinary ME, the correlation time increases approximately exponentially with the volume of the system (Fig. 1*a*, black line). When, in this fast diffusion case, the volume goes to infinity, the rate of escape from an attractor becomes zero. In this macroscopic limit, the system is truly bi-stable.

When the diffusion constants are finite, the τ_c values deviate significantly from those in the homogenous case: when the system volume is small, the correlation times are longer and when the system volume is large, they are shorter than in the homogenous case. The reason why they are longer for small volumes can be traced to the slower reaction kinetics of homogenous systems with finite, as opposed to infinite diffusion rate [33]. The reason why, in large volumes, systems with finite diffusion rates have shorter correlation times than systems with infinite diffusion rates is more interesting: it has to do with domain separations that emerge when the reactants have finite diffusion rates.

For the intermediary diffusion constants (Fig. 1*a*, green and blue lines), the correlation time increases approximately exponentially with the volume, albeit with smaller slopes than in the limit of infinite diffusion rate (Fig. 1*a*, black line). For the smallest diffusion constant, however, the correlation time reaches a plateau where it remains constant, in spite of further volume increase (Fig. 1*a*, red line). Simulations of the total numbers of A and B molecules in the system are also shown in Fig. 1*a* (inserts). At a system volume of $2.5^3\,\mu\text{m}^3$, the distance between the attractors, as measured by the absolute value of the difference between the average numbers of A and B molecules, is largest in the case of infinite diffusion constants and decreases monotonically with decreasing diffusion rates. The reduced difference between the attractors results in ever faster jumps between them.

Further understanding of these events comes from snap-shots showing how the numbers of A (red dots) and B (blue dots) molecules are distributed in a large volume ($V = 6^3\,\mu\text{m}^3$) for systems with slow ($D = 2 \cdot 10^{-9}\,\text{cm}^2\,\text{s}^{-1}$) and intermediate ($D = 5 \cdot 10^{-9}\,\text{cm}^2\,\text{s}^{-1}$) diffusion rates (Fig. 1*b*). Initially, there are only A molecules in the system and in the slow diffusion case, where there is a distinct plateau in Fig. 1*a*, the system rapidly separates into domains of opposite phases. This means that the system is in different attractors in different parts of the volume, which explains

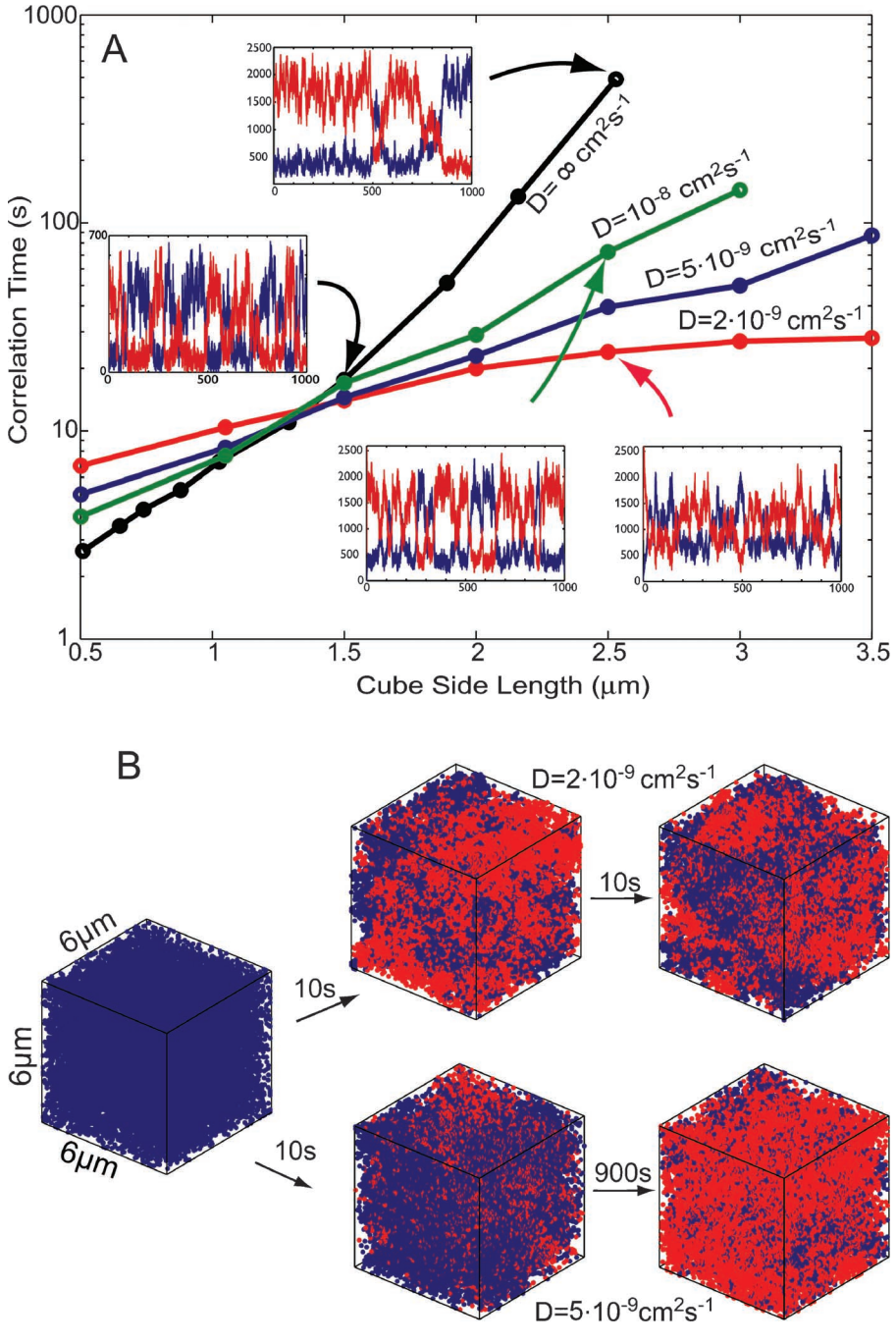

Fig. 1 *Reduction of escape time and domain separation*

a Correlation times of A molecules is plotted for different volumes and diffusion constants. Example of time evolution of the total number of free A and B molecules are given for the points indicated by arrows

b Snap-shots of positions of A and B molecules some times after an initial condition with only B molecules. The volume is $6 \times 6 \times 6\,\mu\text{m}^3$ and $D = 2 \cdot 10^{-9}\,\text{cm}^2\,\text{s}^{-1}$ and $D = 5 \cdot 10^{-9}\,\text{cm}^2\,\text{s}^{-1}$, respectively

why the bi-stability of the total system is almost lost in this case (Fig. 1*a*, insert from red line).

When D is $5 \cdot 10^{-9}\,\text{cm}^2\,\text{s}^{-1}$ there is no visible domain separation, and yet the system jumps between its attractors at a much faster rate than in the homogenous case with infinitely fast diffusion (Fig. 1*b*, compare also black and blue lines in Fig. 1*a*). Part of this increase in the frequency of transitions between the attractors can be ascribed to the reflecting boundaries. That is, close to the boundaries local fluctuations in molecule numbers away from their averages in the dominating phase are less restrained than at positions distal to the boundaries. This can be seen as patches in the opposite phase near the corners in Fig. 1*b*.

To remove such boundary effects, so that the conditions for domain separation in arbitrarily large systems can be clarified, we have also simulated the behaviour of the system in the same volume as in Fig. 1*b*, but with periodic, rather than reflecting, boundary conditions. The system displays domain separation for $D = 2 \cdot 10^{-9}\,\text{cm}^2\,\text{s}^{-1}$ but not for $D = 4 \cdot 10^{-9}\,\text{cm}^2\,\text{s}^{-1}$ (see online supplementary Fig. 1). This implies that the red curve in Fig. 1*a* for $D = 2 \cdot 10^{-9}\,\text{cm}^2\,\text{s}^{-1}$ stays at the plateau also when $L \to \infty$, whereas the correlation times for the other curves go to infinity.

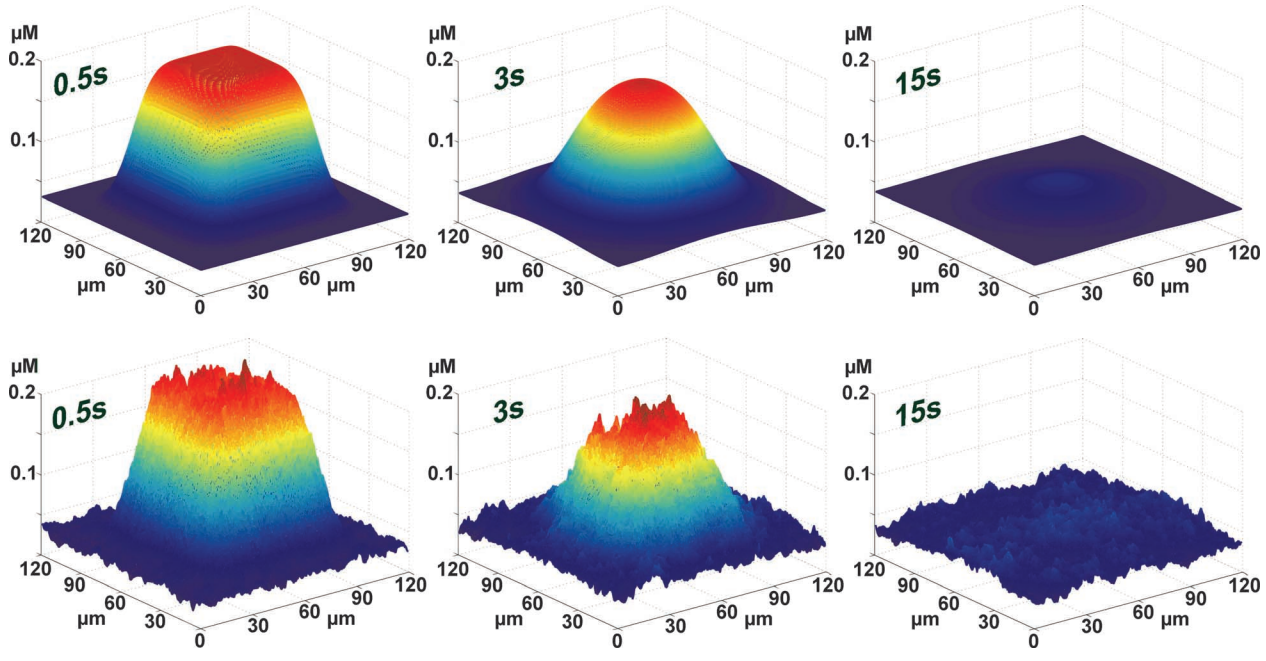

Fig. 2 *The macroscopic approximation in the limit of large D*

The time evolution of the concentrations of A molecules is illustrated by three snap-shots (0.5 s, 3 s and 15 s). The total spatial extension is $120 \times 120 \times 0.6\,\mu m$ and $D = 5 \cdot 10^{-7}\,cm^2\,s^{-1}$

a Solution of macroscopic reaction-diffusion partial differential equations

b Realisation of the same process as described by RDME

2.3 The macroscopic reaction-diffusion equation and curvature of domain fronts

When this bi-stable system is inspected from a macroscopic perspective, the ordinary reaction diffusion equation (see online supplementary text A) allows for stable domains of opposite phases in 1D, but generally not in 2D or 3D. The reason is that a domain with a concave boundary will devour a neighbouring domain with its corresponding convex boundary, and only boundaries that lack curvature can be long-lived [25]. This is illustrated in Fig. 2, where the macroscopic reaction-diffusion equation is integrated for a flat geometry ($120 \times 120 \times 0.6\,\mu m$). The initial condition is that, in a square at the centre of the plane, the system is in the attractor with high concentration of A molecules, and in the remaining part of the volume, the system is in the other attractor (Fig. 2*a*). For comparison, we show a simulation based on the reaction diffusion master equation (Fig. 2*b*). Diffusion is in this case so fast that a large number of molecules are within diffusion range of each other. In this limit, the time evolution of the system is primarily governed by macroscopic laws, and the macroscopic and mesoscopic approaches lead to similar results (Fig. 2). With increasing time, the curvature is eliminated in that the initial square with high A molecule numbers transforms to a circle, which shrinks more and more and eventually disappears.

2.4 The rule for domain separation

What, then, is the rule that determines if a bi-stable system spontaneously separates into spatial domains of different phases? The possibility of domain separation depends, we suggest, on how two different average times react to changes in the total reaction volume V. The first is the correlation time (τ_c) for a homogenous helper system contained in V that is constructed in such a way that all chemical rate constants are identical with those in the real system. That is, the helper system is modelled as homogeneous but with diffusion limited rate constants as in the real system. The correlation time of the helper system will therefore depend both on its volume and the diffusion constants (solid lines in Fig. 3). The second is the time (τ_D) to mix the molecules of the real system in V to homogeneity by diffusion. The mixing time, τ_D, of the real system will depend on the shape of the volume and the rate of diffusion. We suggest that the rule for domain separation is that when $\tau_c \leq \tau_D$ for at least one value of V, domain separation will occur in large systems, but otherwise not.

This type of behaviour is illustrated in Fig. 3 for a system contained in cubic 3D volume V with side length $L = V^{1/3}$. The solid lines are the correlation times (τ_c) for helper systems with reaction rates corresponding to $D = 2 \cdot 10^{-9} cm^2 s^{-1}$ (*black*) and $D = 5 \cdot 10^{-9} cm^2 s^{-1}$

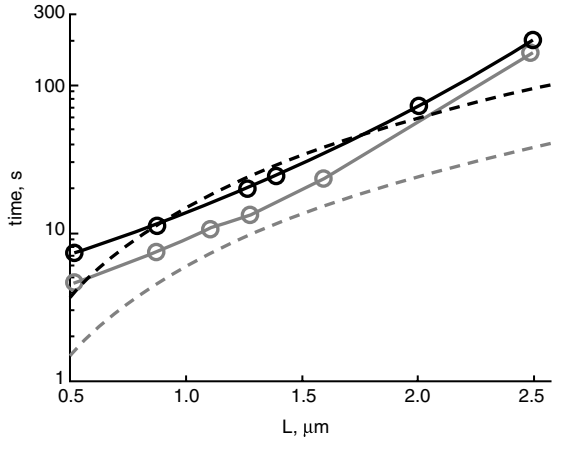

Fig. 3 *The correlation times for homogeneous helper systems of different volumes (L^3) with kinetic parameters corresponding to $D = 2 \cdot 10^{-9}\,cm^2\,s^{-1}$ (black) and $D = 5 \cdot 10^{-9}\,cm^2\,s^{-1}$ (grey) are plotted as solid lines. These are compared to mixing times ($3L^2/D$) of volumes of the same size (dashed). When, for some L, the curves intersect, the system displays domain separation in sufficiently large volumes, but not otherwise*

(*grey*) for the real system. The mixing times (τ_D) required to keep the real systems homogenous by diffusion are proportional [10] to L^2/D with an empirically-estimated constant of proportionality (see online supplementary text C). The τ_D values are plotted versus system volume (dashed lines) for $D = 2 \cdot 10^{-9}\text{cm}^2\text{s}^{-1}$ (*black*) and $D = 5 \cdot 10^{-9}\text{cm}^2\text{s}^{-1}$ (*gray*). When $\tau_c > \tau_D$ for all L, the strong diffusion coupling between neighbouring regions prohibits domain separation. When, in contrast, $\tau_c < \tau_D$ in some interval of L, domain separation is allowed, since the diffusion coupling between neighbouring regions is weak enough to allow for local attractor switches without rapid annihilation of the new phase by the surrounding opposite phase. In Fig. 3, the black curves for $D = 2 \cdot 10^{-9}\text{cm}^2\text{s}^{-1}$ intersect, and in accordance with the suggested rule, the corresponding spatially extended system displays domain separation (Fig. 1*b*). In contrast, the grey curves for $D = 5 \cdot 10^{-9}\text{cm}^2\text{s}^{-1}$ do not intersect and, also in accordance with the rule, there is no domain separation (Fig. 1*b*).

2.5 Diffusion in confined geometries

The cubic 3D volume with side length $L = V^{1/3}$ has a short mixing time compared to a system where the same volume is distributed in a plane with thickness $d \ll V^{1/3}$ and side length $L = (V/d)^{1/2}$ (2D-like system) or in a tube with cross-section d^2 and side length $L = V/d^2$ (1D-like system). In the cubic case the mixing time is proportional to $V^{2/3}/D$, in the 2D-like case to $V/(Dd)$, and in the 1D-like case to $V^2/(Dd^4)$. Since $V^{2/3} \ll V/d \ll V^2/d^4$, it follows that when the same volume V is contained in a thin cylinder, like in a dendrite (1D-like system) [20], or if it is flattened between two membranes (2D-like system), the mixing time is much longer than when V is contained in a spherical or cubic volume (authentic 3D system). This implies that the occurrence of domain separation depends on the shape of the system volume as well as on the diffusion constant and the kinetic parameters that determine τ_j. Fig. 4 illustrates a case when a bi-stable MAPK phosphorylation-dephosphorylation cycle with non-processive, distributed kinase and phosphatase activities [34] displays domain separation in a tube or a flat geometry, but not in a cube. This system is described in more detail in the online supplementary text D.

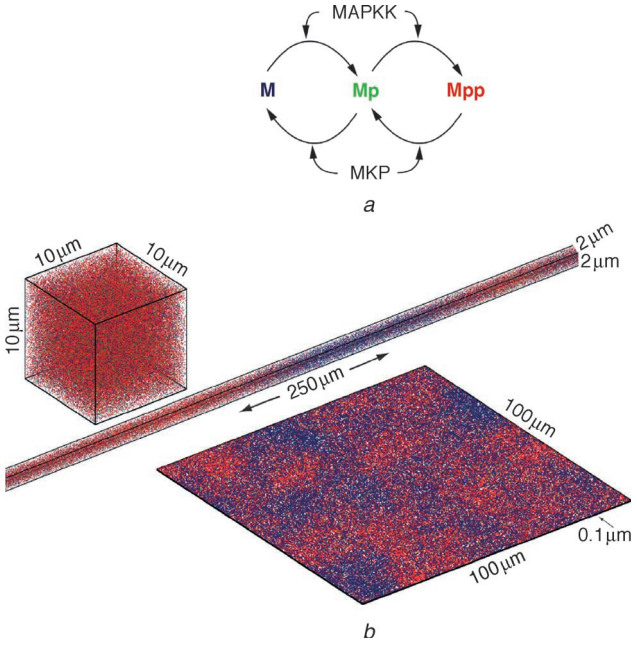

Fig. 4 *The same volume in different geometries*

a A MAPK phosphorylation-dephosphorylation cycle with non-processive, distributed mechanisms for the kinase (MAPKK) and phosphatase (MKP) [34]. The scheme of elementary reactions and the parameters are given in the online supplementary text D

b The system is simulated with $D = 2 \cdot 10^{-8}\ \text{cm}^2\ \text{s}^{-1}$ in a bounded volume of 1000 µm^3 distributed in different geometries. Only 100 µm of the 250 µm tube is shown

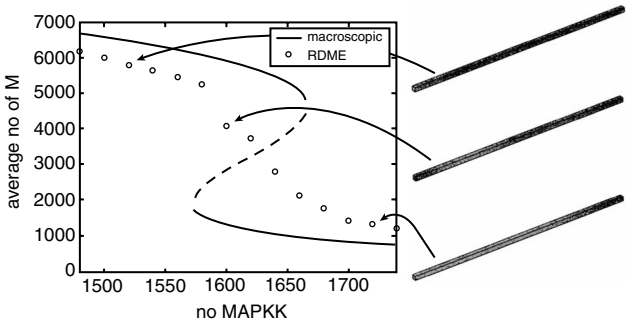

Fig. 5 *Loss of hysteresis in the MAPK system*

X-axis: number of MAPKK molecules in a 54 μm volume. Y-axis: stationary average number of unphosphorylated MAPK (M, black). In a macroscopic model the system displays classical hysteresis when the concentration of MAPKK increases and all other concentrations are kept constant (*line*). When the same system is simulated from the RDME in a $1 \times 1 \times 54\ \mu m$ volume with $D = 2 \cdot 10^{-8}\ cm^2\ s^{-1}$, we see a gradual change in the number of M in the whole volume (*circles*). Snap-shots of the system state are indicated for some of the MAPKK concentrations

2.6 Asymmetric bi-stable systems and hysteresis

So far, we have described symmetric systems where the attractors are equally stable. We will finally illustrate what happens if the MAPK system is made asymmetric by varying the concentration of MAPKK. Macroscopically, the MAPK will display hysteresis [2, 34] as demonstrated in Fig. 5 (*line*). This means that the system can reach different steady states depending on initial conditions and that the state not is reversible for all changes in MAPKK concentration. Likewise, when the conditions for spontaneous domain separation are not fulfilled, the system will display global hysteresis also in a mesoscopic model at a timescale that is faster than the escape rates from the attractors.

However, when spontaneous domain separation emerges, global hysteresis is lost. Instead, the average fraction of the volume that is in one attractor is changed when the concentration of MAPKK is varied over the bi-stable region, so that the average number of phosphorylated molecules in the whole volume changes gradually (Fig. 5). Locally, however, the systems may display hysteresis.

An equivalent loss of global hysteresis due to local fluctuations was recently demonstrated experimentally in inorganic surface catalysis [13].

3 Discussion

With the help of a new and highly efficient Monte Carlo algorithm adapted for the reaction-diffusion master equation we have analysed the stochastic behaviour of bi-stable systems in 3D. The results suggest general rules for when those systems separate into spatial domains of opposite phases. Spontaneous domain separation requires that a localised part of the system jumps from an attractor in phase to an attractor out of phase with the surroundings. For this to happen, the size of the part of the system that jumps out of phase must be big enough so that it is not invaded by

neighbouring molecules. At the same time, the size must be small enough so that the local escape from the original attractor does not take too long. It is only when there exists a local volume size for which invasion by diffusion takes a longer time than attractor escape, that spatial domains become sufficiently decoupled from their surroundings to allow for spontaneous domain separation. Accordingly, systems in tube-like or flat geometries display domain separation much more easily than do their spherical or cubic equivalents. Furthermore, geometric restrictions in small reaction volumes, like intracellular membrane structures, will reduce attractor escape times in localised areas which will strongly promote the emergence of spatial domains in opposite phases. This eliminates hysteresis in the total cell volume, meaning that absence of hysteresis cannot be used to infer lack of intrinsic bi-stability of an experimentally studied system [2].

Bi-stable switches in living cells may for their proper function depend on the existence of spatial domains in opposite phase. For instance, long-term potentiation (LTP) in post synaptic dendrites depends on a bi-stable system that separates into domains of opposite phase in a single cell [35, 36]. LTP is maybe partly mediated by phosphorylation of CaMKII following Ca^{2+} release [8, 37]. The phosphorylated state of CaMKII displays hysteresis, in that its activity remains high also after a reduction of the Ca^{2+} concentration [38]. These system properties are intriguing in light of the present results and lead to a number of questions: (i) how can CaMKII in adjacent synapses be in different activity states, when Ca^{2+} spreads through the dendrite? (ii) why is it that activated CaMKII in one synapse does not phopsphorylate CaMKII in neighbouring synapses? (iii) how are spontaneous attractor escapes in local areas avoided? The answers are that the CaMKII system has evolved so that: (i) calcium signalling is isolated in tiny compartments (spines) protruding from the dendrites [39]; (ii) CaMKII can only be active when it is bound to protein scaffolds in the postsynaptic density [38]; (iii) CaMKII is a 12 subunit protein complex with about 30 phosphorylation sites, which makes it resilient to stochastic fluctuations [37].

In other cases, bi-stable control circuits must be in global attractors that extend throughout the whole intracellular space. Such examples are the tightly controlled cell fate decision circuits, which play essential roles in cell cycle regulation [40] and cell maturation [5]. These circuits must be designed so that domain separations do not occur and so that spontaneous attractor escape times are sufficiently long. This can be achieved by slow reaction kinetics in combination with unrestrained intracellular diffusion, ideally in a single, spherical compartment without nooks.

Spatially distributed protein phosphorylation cascades transmit signals from membrane-bound receptors to cytosolic targets [41]. These signal molecules are phosphorylated by membrane-bound kinases and dephosphorylated by cytosolic phosphatases, which can lead to concentration gradients and low signal strength in the target region [42]. It has been suggested that bi-stable signal systems could overcome this problem by their ability to maintain high signal strengths over long distances [43]. The proposed mechanism is attractive, but depends critically on the absence of local spontaneous state changes along communication channels from membrane receptor to target. This requires high signal molecule concentrations and free diffusion from signal source to signal target, unhindered by narrow passages or partially isolated compartments.

4 Acknowledgments

We thank Otto Berg, Upinder Bhalla, James Ferrell, Dan Gillespie, Malek Mansour, and Johan Paulsson for helpful comments on the manuscript. The work was supported by the National Graduate School of Scientific Computing and the Swedish Research Council.

5 References

1 Monod, J., and Jacob, F.: 'General conclusions: teleonomic mechanisms in intracellular metabolism, growth, and differentiation', *Cold Spring Harbour Symp. Quant. Biol.*, 1961, **26**, pp. 389–401
2 Ferrell, J.E., Jr.: 'Self-perpetuating states in signal transduction: positive feedback, double-negative feedback and bistability', *Current Opinion in Cell Biology*, 2002, **14**, pp. 140–148
3 Angeli, D., Ferrell, J.E., Jr., and Sontag, E.D.: 'Detection of multistability, bifurcations, and hysteresis in a large class of biological positive-feedback systems', *Proc. Natl. Acad. Sci. USA*, 2004, **101**, pp. 1822–1827
4 Tyson, J.J., Chen, K., and Novak, B.: 'Network dynamics and cell physiology', *Nat. Rev. Mol. Cell. Biol.*, 2001, **2**, pp. 908–916
5 Xiong, W., and Ferrell, J.E., Jr.: 'A positive-feedback-based bistable 'memory module' that governs a cell fate decision', *Nature*, 2003, **426**, pp. 460–465
6 Becskei, A., Seraphin, B., and Serrano, L.: 'Positive feedback in eukaryotic gene networks: cell differentiation by graded to binary response conversion', *Embo. J.*, 2001, **20**, pp. 2528–2535
7 Bhalla, U.S., Ram, P.T., and Iyengar, R.: 'MAP kinase phosphatase as a locus of flexibility in a mitogen-activated protein kinase signaling network', *Science*, 2002, **297**, pp. 1018–1023
8 Bhalla, U.S., and Iyengar, R.: 'Emergent properties of networks of biological signaling pathways', *Science*, 1999, **283**, pp. 381–387
9 Gardiner, C.: 'Handbook of stochastic methods' (Springer-Verlag, Berlin, 1985, 2nd edn.)
10 Van Kampen, N.G.: 'Stochastic processes in physics and chemistry' (Elsevier, Amsterdam, 1997, 2nd edn.)
11 Shapiro, L., and Losick, R.: 'Dynamic spatial regulation of the bacterial cell', *Cell*, 2000, **100**, pp. 89–98
12 Batada, N.N., Shepp, L.A., and Siegmund, D.O.: 'Stochastic model of protein-protein interaction: why signaling proteins need to be colocalized', *Proc. Natl. Acad. Sci. USA*, 2004, **101**, pp. 6445–6449
13 Johanek, V., Laurin, M., Grant, A.W., Kasemo, B., Henry, C.R., and Libuda, J.: 'Fluctuations and bistabilities on catalyst nanoparticles', *Science*, 2004, **304**, pp. 1639–1644
14 Paulsson, J.: 'Summing up the noise in gene networks', *Nature*, 2004, **427**, pp. 415–418
15 Korobkova, E., Emonet, T., Vilar, J.M., Shimizu, T.S., and Cluzel, P.: 'From molecular noise to behavioural variability in a single bacterium', *Nature*, 2004, **428**, pp. 574–578
16 McQuarrie, D.A.: 'Stochastic approach to chemical kinetics', *J. Appl. Probab.*, 1967, **4**, pp. 413–478
17 Elowitz, M.B., Surette, M.G., Wolf, P.E., Stock, J.B., and Leibler, S.: 'Protein mobility in the cytoplasm of Escherichia coli', *J Bacteriol.*, 1999, **181**, pp. 197–203
18 Howard, M., and Rutenberg, A.D.: 'Pattern formation inside bacteria: fluctuations due to the low copy number of proteins', *Phys. Rev. Lett.*, 2003, **90**, p. 128102
19 Turing, A.M.: 'The chemical basis of morphogenesis', *Philos. Trans. R. Soc. Lond.*, 1952, **237**, pp. 37–72
20 Finch, E.A., and Augustine, G.J.: 'Local calcium signaling by inositol-1,4,5-trisphosphate in Purkinje cell dendrites', *Nature*, 1998, **396**, pp. 753–756
21 Thar, R., and Kuhl, M.: 'Bacteria are not too small for spatial sensing of chemical gradients: an experimental evidence', *Proc. Natl. Acad. Sci. USA*, 2003, **100**, pp. 5748–5753
22 Nicolis, G., and Prigogine, I.: 'Self-organization in nonequilibrium systems' (John Wiley, New York, 1977)
23 Baras, F., and Mansour, M.M.: 'Microscopic simulation of chemical instabilities', *Adv. Chem. Phys.*, 1997, **100**, pp. 393–475
24 Gorecki, J., Kawaczynski, A.L., and Nowakowski, B.: 'Master equation and molecular dynamics simulations of spatiotemporal effects in a bistabile chemical system', *J. Phys. Chem. A*, 1999, **103**, pp. 3200–3209
25 Mikhailov, A.: 'Foundations of synergetics I', in Haken, H. (Ed.): (Springer Verlag, Berlin, 1990)
26 Meerson, B.: 'Domain stability, competition, growth, and selection in globally constrained bistabile systems', *Phys. Rev. E*, 1996, **53**, pp. 3491–3494
27 Gillespie, D.: 'A general method for numerically simulating the stochastic time evolution of coupled chemical reactions', *J. Comput. Phys.*, 1976, **22**, pp. 403–434
28 Malek-Mansour, M., and Houard, J.: 'A new approximation scheme for the study of fluctuations in nonuniform nonequilibrium systems', *Phys. Lett. A*, 1979, **70**, pp. 366–368
29 Andér, M., Beltrao, P., Di Ventura, B., Ferkinghoff-Borg, J., Foglierini, M., Kaplan, A., Lemerle, C., Tomas-Oliveira, I., and Serrano, L.: 'SmartCell: a framework to simulate cellular processes that

combines stochastic approximation with diffusion and localisation: analysis of simple gene networks', *Systems Biology*, 2004, **1**
30 Andér, M.: 'SmartCell - a general framework for whole cell modelling and simulation', *UPTEC X 02 021*, 2002, http://www.ibg.uu.se/upload/2002-11-18_162646_535/Maria_A.pdf
31 Kaplan, A.: 'On whole-cell modelling and simulation', *UPTEC X 01 044*, ISSN 1401-2138 2001, http://www.ibg.uu.se/upload/2002-07-10_225930_995/01044.pdf
32 Gibson, M., and Bruck, J.: 'Efficient exact stochastic simulation of chemical systems with many species and channels', *J Phys. Chem. A*, 2000, **104**, pp. 1876–1889
33 Berg, O.G.: 'On diffusion-controlled dissociation', *Chem. Phys.*, 1978, **31**, pp. 47–57
34 Markevich, N.I., Hoek, J.B., and Kholodenko, B.N.: 'Signaling switches and bistability arising from multisite phosphorylation in protein kinase cascades', *J Cell. Biol.*, 2004, **164**, pp. 353–359
35 Koch, C.: 'Biophysics of computation' (Oxford University Press, New York, 1999)
36 Lisman, J.E.: 'A mechanism for memory storage insensitive to molecular turnover: a bistable autophosphorylating kinase', *Proc. Natl. Acad. Sci. USA*, 1985, **82**, pp. 3055–3057
37 Lisman, J.E., and Goldring, M.A.: 'Feasibility of long-term storage of graded information by the Ca2+/calmodulin-dependent protein kinase molecules of the postsynaptic density', *Proc. Natl. Acad. Sci. USA*, 1988, **85**, pp. 5320–5324
38 Lisman, J.E., and Zhabotinsky, A.M.: 'A model of synaptic memory: a CaMKII/PP1 switch that potentiates transmission by organizing an AMPA receptor anchoring assembly', *Neuron*, 2001, **31**, pp. 191–201
39 Augustine, G.J., Santamaria, F., and Tanaka, K.: 'Local calcium signaling in neurons', *Neuron*, 2003, **40**, pp. 331–346
40 Sha, W., Moore, J., Chen, K., Lassaletta, A.D., Yi, C.S., Tyson, J.J., and Sible, J.C.: 'Hysteresis drives cell-cycle transitions in Xenopus laevis egg extracts', *Proc. Natl. Acad. Sci. USA*, 2003, **100**, pp. 975–980
41 Chang, L., and Karin, M.: 'Mammalian MAP kinase signalling cascades', *Nature*, 2001, **410**, pp. 37–40
42 Kholodenko, B.N.: 'MAP kinase cascade signaling and endocytic trafficking: a marriage of convenience?', *Trends Cell. Biol.*, 2002, **12**, pp. 173–177
43 Kholodenko, B.N.: 'Four-dimensional organization of protein kinase signaling cascades: the roles of diffusion, endocytosis and molecular motors', *J. Exp. Biol.*, 2003, **206**, pp. 2073–2082